Reacting to outbreaks at neighboring localities

Ceyhun Eksin[a,b,*], Martial-Ndeffo Mbah[c], Joshua S. Weitz [d,e,f]

[a] *Industrial and Systems Engineering Department, Texas A&M University, College Station, TX, USA*
[b] *Electrical and Computer Engineering Department, Texas A&M University, College Station, TX, USA*
[c] *College of Veterinary Medicine and Biomedical Sciences, Texas A&M University, College Station, TX, USA*
[d] *School of Biological Sciences, Georgia Institute of Technology, Atlanta, GA, USA*
[e] *School of Physics, Georgia Institute of Technology, Atlanta, GA, USA*
[f] *Center for Microbial Dynamics and Infection, Georgia Institute of Technology, Atlanta, GA, USA*

Abstract

We study the dynamics of epidemics in a networked metapopulation model. In each subpopulation, representing a locality, disease propagates according to a modified susceptible-exposed-infected-recovered (SEIR) dynamics. We assume that individuals reduce their number of contacts as a function of the weighted sum of cumulative number of cases within the locality and in neighboring localities. We also assume that susceptible and exposed (pre-symptomatic and infectious) individuals can travel between localities. To investigate the combined effects of mobility and contact reduction on disease progression within interconnected localities, we consider a scenario with two localities where disease originates in one and is exported to the neighboring locality via travel of undetected pre-symptomatic individuals. We establish a lower bound on the outbreak size at the origin as a function of the speed of spread. We associate the behavior change at the disease-importing locality due to the outbreak size at the origin with the level of preparedness of the locality. Using the lower bound on the outbreak size at the origin, we establish an upper bound on the outbreak size at the importing locality as a function of the speed of spread and the level of preparedness for low mobility regimes. We show the accuracy of the bounds in determining critical levels of preparedness that stop the disease from becoming endemic at neighboring localities. Finally, we show how the benefit of preparedness diminishes under high mobility rates. Our results highlight the importance of preparedness at localities where cases are beginning to rise, and demonstrate the benefits of increase in contact reduction by considering the outbreaks in neighboring localities with severe, rather than weak, outbreaks.

Keywords: Epidemiology, networked metapopulation, nonlinear dynamics, social distancing.

1. Introduction

Early detection of disease outbreaks at their location of origin provide a chance for local containment and time to prepare in other locations. Such preparation may enable locations connected to the origin to become more aware of the outbreak and develop a stronger response to the disease especially when it is not contained. The success of containment strategies is highly dependent on the ability of promptly detecting most infectious individuals in a given location. The recent outbreak of the COVID-19 virus has shown that successful containment efforts are highly challenging when many infectious individuals remain asymptomatic and can travel undetected between locations [1].

In the ongoing COVID-19 outbreak, localities in the US are beginning to see alarming surges in their number of cases and hospitalized individuals at different times, likely because the introduction times of the disease to the local communities differ [2]. While reducing mobility between localities can delay the overall epidemic progression, the epidemic trajectory, e.g., the final outbreak size, is not strongly affected by the travel restrictions unless they are combined with a strong reduction in transmission within the locality [3, 4, 5, 6]. In the US, local authorities are implementing non-pharmaceutical interventions, e.g., declaring emergency or issuing stay at home orders, at different

*Correspondence to eksinc@tamu.edu

times. Community response to these interventions differ across localities [7]. The premise of this work is to assess— in a generalized model —the combined effects of mobility, local response to disease prevalence, and the level of alertness prior to disease surge in a locality.

Here, we consider a networked-metapopulation model [8, 9, 10, 11] where the disease progresses according to susceptible-exposed-infected-recovered (SEIR) dynamics within each population or locality (similar to [12]). Within each population, susceptible individuals can become exposed, i.e., pre-symptomatic, by being in contact with individuals in exposed and infected compartments. Recent experiments on temporal viral shedding of COVID-19 estimate near half of the secondary cases happen by being in contact with individuals in pre-symptomatic stage [13]. The difference between pre-symptomatic infected and infected individuals is that pre-symptomatic individuals can travel between localities undetected. In our model, the exposed individuals progress to being infected and then to being recovered. That is, we do not make a distinction between symptomatic and asymptomatic infected individuals; further extensions could incorporate such differences, e.g., [1, 14].

Our focus is on the role of behavior changes in different localities and the effects of behavior changes on local disease progression. We assume individuals change their behavior and reduce their contacts proportional to disease severity, i.e., the ratio of infected and recovered, in the population [15, 16]. In addition, behavior in a locality can be affected by the disease severity in neighboring localities. That is, individuals in a locality take protective measures, e.g., social distancing, based on disease severity in a neighboring locality. In particular, we consider a scenario between two localities in which the disease originates in one, and moves to the other locality by mobility of exposed individuals. In this scenario, we interpret initial behavior changes at the locality neighboring the origin as 'preparedness-based' behavior change. Our aim is to quantify the combined effects of inter-locality mobility, preparedness-based behavior change, and behavior changes in response to local disease prevalence. Our analysis focuses on delay in peak times between two localities, total outbreak size and the outbreak size at localities neighboring the origin as a function of mobility, preparedness, and population response.

2. Methods

We consider a networked meta-population model. At each population, the disease propagates according to SEIR dynamics, that assumes a homogeneously mixed population. In addition, we assume there is constant travel in and out of each population. At midst of containment efforts, the flow of travelers constitute only healthy (susceptible) individuals, and those that are infectious without symptoms (exposed). The dynamics at locality i is given as follows:

$$\dot{S}_i = -\beta_i \frac{S_i(I_i + E_i)}{N_i} + \sum_{j\in\mathcal{N}_i} \lambda_{ji} \frac{S_j}{S_j + E_j} - \frac{S_i}{S_i + E_i} \sum_{j\in\mathcal{N}_i} \lambda_{ij} \quad (1)$$

$$\dot{E}_i = \beta_i \frac{S_i(I_i + E_i)}{N_i} - \mu E_i + \sum_{j\in\mathcal{N}_i} \lambda_{ji} \frac{E_j}{S_j + E_j} - \frac{E_i}{S_i + E_i} \sum_{j\in\mathcal{N}_i} \lambda_{ij} \quad (2)$$

$$\dot{I}_i = \mu E_i - \delta I_i \quad (3)$$

$$\dot{R}_i = \delta I_i, \quad (4)$$

where β_i is the transmission rate at location i, λ_{ij} is the flow of individuals from location i to neighboring location j, μ denotes transition rate from exposed (pre-symptomatic) to infected (symptomatic), and δ is the recovery rate. We denote the neighboring localities of i with $\mathcal{N}_i$. We assume total flow in and out of a location are equal, i.e., $\lambda_{ij} = \lambda_{ji}$. The total mobility flow from i to j include susceptible and exposed individuals proportional to their size in the population. We assume infected individuals cannot move without being detected.

The transmission rate at location i depends on the inherent infectivity rate β_0 and social distancing due to disease prevalence,

$$\beta_i = \beta_0 \left(1 - \omega_{ii} \frac{I_i + R_i}{N_i} - \sum_{j\in\mathcal{N}_i} \omega_{ij} \frac{I_j + R_j}{N_j}\right)^{\alpha_i}. \quad (5)$$

In the social distancing model, individuals reduce their interaction with others proportional to the ratio of cumulative cases, defined as the ratio of infectious and recovered in the population, at locality i and neighboring localities of i [15, 16, 17]. The term inside the parentheses is the awareness at locality i caused by disease prevalence. The weight

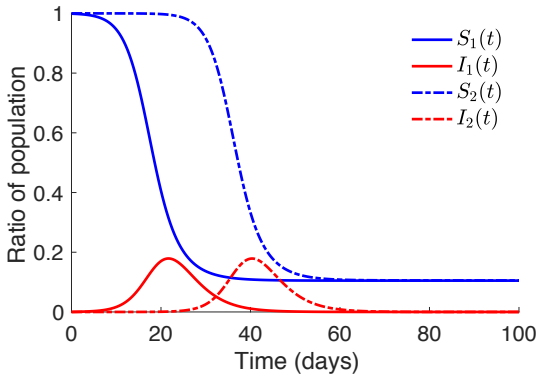

Figure 1: Networked SEIR model with no-distancing. Two localities are connected with travel rates $\lambda_{ij} = 0.01\%$. The disease propagates in both localities according to SEIR dynamics with no response to disease prevalence, i.e., $\alpha_i = 0$. Blue and red lines show the ratio of susceptible and infected individuals in a locality, respectively. The difference in time of peaks is 19 days. Final outbreak sizes of localities 1 and 2 are almost identical.

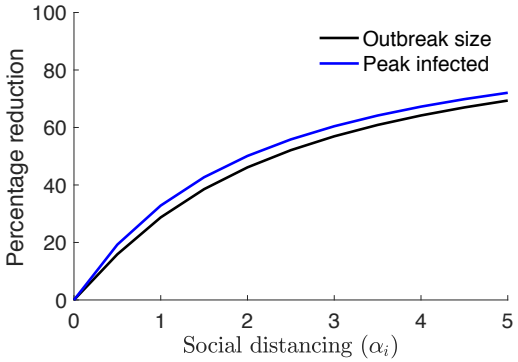

Figure 2: Percentage reduction in outbreak size and ratio of infected at peak with respect to increasing social distancing exponent (α_i). We measure the reduction with respect to the no-distancing case ($\alpha_i = 0$). In both cases, we have the mobility per day $\lambda_{12} = \lambda_{21} = 0.01\%$ of the population.

constant $\omega_{ii} \in [0, 1]$ determines the importance of disease prevalence at locality i versus the importance of disease prevalence at neighboring $\mathcal{N}_i$ localities, $\omega_{ij} \in [0, 1]$. We assume the weights sum to one, i.e., $\sum_{j \in \mathcal{N}_i \bigcup i} \omega_{ij} = 1$. The exponent constant α_i represents the strength of response to the disease awareness. It determines the overall distancing at locality i based on the awareness. If $\alpha_i = 0$, there is no distancing response to the awareness at locality i. Note that the awareness term inside the parentheses is always less than or equal to 1. Thus, the larger α_i is, the larger is the distancing response at locality i to disease prevalence. We refer to the case with $\alpha_i = 1$ as the linear distancing model.

In the following, we consider two localities with equal population sizes $N_1 = N_2$. The disease starts at locality 1 with 0.1% infected, and spreads over to locality 2 via undetected exposed individuals traveling from 1 to 2. We set $\beta_0 = \frac{1}{2}$, $\mu = \frac{1}{2}$, and $\delta = \frac{1}{3}$ based on the rates estimated at [1] for the COVID-19 outbreak in China. The reproduction number is equal to 2.5. Note that we have the standard SEIR model in both localities when $\alpha_i = 0$ and $\lambda_{ij} = 0$ for all localities.

3. Results

3.1. Mobility and Social Distancing

As a baseline we consider no distancing response, i.e., $\alpha_i = 0$ for all $i = \{1, 2\}$—see Figure 1. We find that the Locality 2 goes through an almost identical disease trajectory as Locality 1 approximately 19 days after Locality 1 in this scenario. The difference in peak times of two localities increases from 8 days to 27 days as λ_{ij} decreases from 1% to 0.001%. Next, we consider the effect of social distancing. For this, we assume localities only put weight on disease prevalence at their own locality, i.e., $\omega_{ii} = 1$ for $i \in \{1, 2\}$. Figure 2 shows the percentage reduction in final outbreak size and peak ratio of infected at Locality 2 as localities become more responsive, i.e., as α_i increases. When the distancing is linear $\alpha_i = 1$, the reductions in peak and outbreak size are near 25%. Reduction in both metrics reaches above 60% when $\alpha_i = 5$. While both metrics continue to decrease with α_i increasing, there does not exist a critical threshold of α_i that stops the outbreak from happening [15]. This is due to the proportionality of the social distancing to the cumulative number of cases.

In the following we characterize the effects of social distancing with respect to local disease prevalence and strength of response (α_i) on the outbreak size of the origin.

3.2. A lower bound on the outbreak size at the origin

We provide a speed of spread and final size relation whose solution yields a lower bound for the outbreak size at the origin in a scenario without

mobility ($\lambda_{ij} = 0$) and $\omega_{12} = 0$,

$$S(\infty) - \left(1 + \alpha_1 \mathcal{R}_1 (1 - S(\infty))\right)^{-\frac{1}{\alpha_1}} = 0, \quad (6)$$

where $\mathcal{R}_1$ is the reproductive number at the origin given by

$$\mathcal{R}_1 = \beta_0 \left(\frac{1}{\delta} + \frac{1}{\mu}\right). \quad (7)$$

In obtaining the relation in (6), we consider a SEIR model with a modified social distancing model in which we also include fraction of exposed E in the distancing term—see Appendix A. When individuals reduce their interactions proportional to the cumulative number of exposed cases, the social distancing is stronger than (5). Thus the solution to (6) for the final susceptible ratio in the population is an *upper bound* for the final susceptible ratio in the SEIR model above (1)-(5). For $\alpha_1 = 1$, we get a close-form solution to (6),

$$S(\infty) = \mathcal{R}_1^{-1}, \; R(\infty) = 1 - \mathcal{R}_1^{-1}. \quad (8)$$

Figure 3 compares the actual outbreak sizes with the upper bound for $S(\infty)$ obtained by solving (6) for different values of α_1. We observe that the upper bound solution, denoted with ($\hat{S}(\infty)$), is loose by a constant amount that is approximately equal to 0.04 in both $k = 1$ and $k = 3$. We also note that this upper bound is also a good approximation of the outbreak size at Locality 2 when mobility is low and $\omega_{22} = 1$.

Thus far, our analysis focused on the effects of social distancing measures taken based on disease prevalence at the locality. In the following, we consider the effects of distancing measures when they are based on the disease prevalence (outbreak size) at neighboring localities.

3.3. Adopted awareness

We analyze the effect of awareness at Locality 2 caused by the outbreak in Locality 1. We denote the weight ω_{21} associated with this awareness as the adopted awareness weight. Locality 1, the origin of the outbreak, faces the outbreak first. We assume Locality 1's awareness is not shaped by the outbreak at Locality 2, i.e., $\omega_{11} = 1$. In this scenario, the adopted awareness should be interpreted as individuals in Locality 2 reducing contacts, i.e., practice social distancing, based on the awareness created by the outbreak at Locality 1. When the

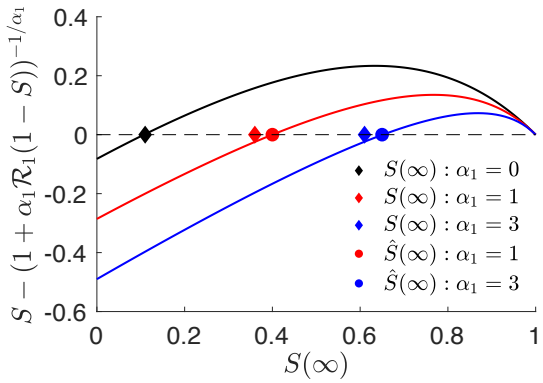

Figure 3: Upper bound values of $S(\infty)$ obtained by solving (6) for $k = 1$ and $k = 3$. We let $\mathcal{R}_1 = 2.5$. Lines correspond to the left hand side of (6). Circle dots show the solution to (6). Diamond dots are $S(\infty)$ values obtained by simulating the SEIR model in (1)-(4) with β_i given in (5). For $k = 0$, we use standard speed-size relations for the SEIR model without social distancing [18]. Note that the relation for the standard SEIR model is exact. Thus, diamond and circle dots overlap for $k = 0$. The difference between the upper bound for $S(\infty)$ ($\hat{S}(\infty)$) and the simulated $S(\infty)$ is relatively constant for different values of α_1.

disease starts in one location (Locality 1) and moves to a neighboring locality (Locality 2) via travel of exposed or asymptomatic infectious individuals from the origin, the adopted awareness distancing term at Locality 2 is a measure of its preparedness.

We begin by using the lower bound for the outbreak size at the origin ($\hat{R}_1(\infty)$) to obtain an upper bound for the outbreak size at Locality 2 as a function of ω_{21}. There exists a time $T > 0$ such that for all $t > T$, we have $\hat{R}_1(\infty) < I_1(t) + R_1(t)$ where $\hat{R}_1(\infty)$ is obtained by solving (6) for $\hat{S}_1(\infty)$ and setting $\hat{R}_1(\infty) = 1 - \hat{S}_1(\infty)$. Consider the social distancing model $\beta_2(t)$ in (5). For $t > T$, we have

$$\beta_2(t) < \beta_0 \left(1 - \omega_{21} \hat{R}_1(\infty) - \omega_{22}(I_2 + R_2)\right)^{\alpha_2}. \quad (9)$$

As mobility slows down, i.e., $\lambda_{12} \to 0$, the threshold time T approaches zero as well. Thus, in the slow mobility regime, the inequality above holds for almost all times. By getting rid of the social distancing based on local awareness, we obtain the following upper bound on the infection rate at the importing locality (Locality 2),

$$\beta_2(t) < \beta_0 \left(1 - \omega_{21} \hat{R}_1(\infty)\right)^{\alpha_2}. \quad (10)$$

Note that the right hand side is a constant that

depends on the lower bound of the outbreak size at the origin and the strength of response at Locality 2 (α_2). Given the constant upper bound in (10), we use the speed-outbreak size relation for the standard SEIR model, e.g., see [18, 19], to obtain a lower bound for $S(\infty)$,

$$1 - \tilde{S}(\infty) + \tilde{\mathcal{R}}_2^{-1} \log(\tilde{S}(\infty)) = 0. \tag{11}$$

where we define

$$\tilde{\mathcal{R}}_2 := \beta_0 \left(1 - \omega_{21} \hat{R}_1(\infty)\right)^{\alpha_2} \left(\frac{1}{\delta} + \frac{1}{\mu}\right). \tag{12}$$

The solution to (11) given by $\tilde{S}(\infty)$ provides a lower bound for $S(\infty)$ in the SEIR model with social distancing (1)-(5). Note that we obtain the speed-outbreak size relation for the standard SEIR model when $\alpha_2 = 0$. In Appendix B, we demonstrate how the solution changes in the lower bound as a function of strength of responses at localities—see Figures S1-S2.

In Figure 4 we compare the outbreak size at Locality 2 from simulating (1)-(5) with the upper bound obtained by solving (11) for a range of adopted awareness values $\omega_{21} \in [0, 1]$. We observe that the upper bound is loose when the adopted awareness is close to zero. This is reasonable since in deriving the bound we removed the social distancing with respect to local disease prevalence. The accuracy of the upper bound improves as the adopted awareness constant increases. Indeed, as per our assumptions, as $\lambda_{21} \to 0$, the upper bound would tend to the actual outbreak size when $\omega_{22} = 0$.

Figure 4 also shows that the outbreak size at Locality 2 and the associated upper bound monotonically decreases as adopted awareness (w_{21}) increases for the given strengths of response at the origin $\alpha_1 \in \{1, 3\}$. This means Locality 2 is better off reacting to the outbreak at Locality 1, as this will lead to an early strong response to the disease. Indeed, the decrease of the outbreak size at Locality 2 with respect to the adopted awareness constant is faster when the response at Locality 1 is weak—compare blue and black lines within Top and Bottom figures. The reason for this is that a weaker response at Locality 1 results in a higher ratio of cumulative cases, which means higher awareness at Locality 2. Going in the other direction, if the strength of response at Locality 1 further increases ($\alpha_1 > 3$), it is possible that increasing adopted awareness increases the outbreak size at Locality 2.

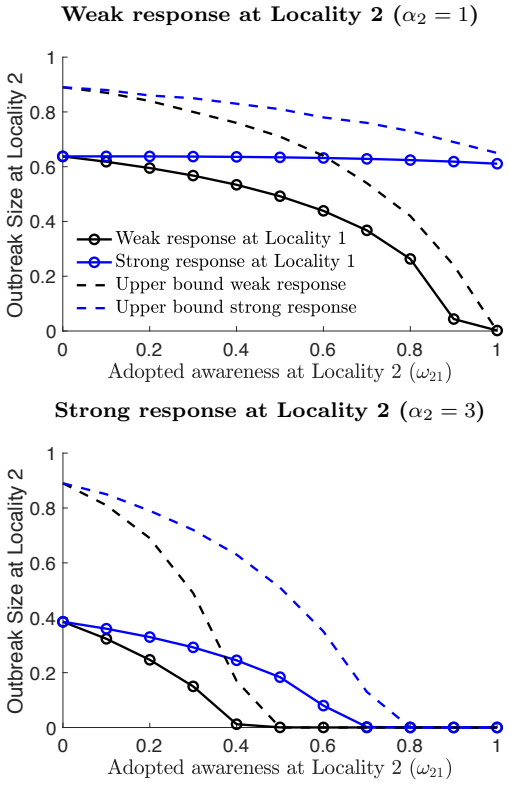

Figure 4: Outbreak size at Locality 2 with respect to adopted awareness ω_{21}. (Top) Weak ($\alpha_2 = 1$) and (Bottom) Strong ($\alpha_2 = 3$) responses at Locality 2. Mobility is set to $\lambda = 0.001\%$. Weak and strong responses at Locality 1 correspond to $\alpha_1 = 1$ (black) and $\alpha_1 = 3$ (blue), respectively. The outbreak size at Locality 2 decreases with increasing adopted awareness values. The decrease is sharper when response at the origin is weak. Corresponding theoretical upper bound values (shown by dashed lines) are tighter at larger adopted awareness values. In the Bottom figure, the critical threshold values ω_{21}^* above which disease does not propagate approximately equal to 0.5 and 0.8 respectively for weak (black) and strong (blue) responses at the origin.

This means the monotonic decrease in the outbreak size at Locality 2 with respect to increasing adopted awareness is contingent on the strength of response at Locality 1 and the mobility constants.

The preparedness at Locality 2 can result in stopping the disease from becoming endemic at Locality 2. Indeed, we observe in Figure 4 (Bottom) that there exists a critical threshold for the adopted awareness constant $w_{21} > 0.4$ above which outbreak size is near zero for Locality 2. Next, we use the upper bound for the outbreak size at Locality 2 to compute an upper bound for the critical threshold value of the adopted awareness constant for a given α_1 and α_2 value.

In order to obtain this threshold, we rely on the result that when $\mathcal{R}_2 < 1$, the disease will die out in a standard SEIR model. Note that $\mathcal{R}_2 < \tilde{\mathcal{R}}_2$ with $\tilde{\mathcal{R}}_2$ is as defined in (12). Thus, disease at Locality 2 will not become endemic if $\tilde{\mathcal{R}}_2 < 1$. Solving this condition for ω_{21}, we get the following threshold

$$\omega_{21} > \frac{1 - \mathcal{R}_1^{-1/\alpha_2}}{\hat{R}_1(\infty)} \tag{13}$$

where $\mathcal{R}_1$ is the reproductive number (7) and $\hat{R}_1(\infty)$ is the lower bound on the outbreak size at the origin obtained by solving (6). From (13), we see that the critical threshold value for adopted awareness (ω_{21}^*) increases with increasing α_1 and decreases with increasing α_2. In Figure 4 (Bottom), we see that the theoretical critical threshold values are close to the actual (simulated) ω_{21} values above which the disease does not propagate in Locality 2.

For $\alpha_1 = 1$, we obtain a close form solution for $\hat{R}_1(\infty)$ in (8), which yields

$$\omega_{21} > \frac{1 - \mathcal{R}_1^{-1/\alpha_2}}{1 - \mathcal{R}_1^{-1}}. \tag{14}$$

The threshold value above is an increasing function of α_2. That is, Locality 2 can avoid an outbreak with a smaller adopted awareness constant (ω_{21}) as α_2 increases. For $\alpha_2 = 1$, we have the right hand side equal to 1. This means there does not exist a level of preparedness, i.e., a value of $\omega_{21} \in [0, 1]$, such that the disease is eliminated at Locality 2. This confirms the results shown in Figure 4 (Top)—see solid and dashed black lines decreasing toward 0 as ω_{21} goes to 1. At $\omega_{21} = 1$, we are right at the boundary where the upper bound on the outbreak size is close to, but not equal to, zero.

3.4. Effect of adopted awareness on total outbreak size

While the above analyses show that Locality 2 can benefit from a heightened awareness due to a weak response at Locality 1, this awareness is a direct result of the lack of control at Locality 1. Indeed, a larger outbreak at Locality 1 yields a lower outbreak size at Locality 2. Here, we answer under what conditions the reduction in the outbreak size at Locality 2 due to the increase in the outbreak size at Locality 1 is larger than the increase in the outbreak size at Locality 1.

We begin by focusing on the total outbreak size defined as the sum of outbreak sizes in both localities, i.e., $R_1(\infty) + R_2(\infty)$, as a global measure of the effects of adopted awareness. In Figure 5 (Top), we find that when the response at Locality 2 is weak ($\alpha_2 = 1$), there exists a level of preparedness ($\omega_{21} \approx 0.7$) above which the total outbreak size is smaller when the response at Locality 1 is weak—see blue line dip below the black line around $\omega_{21} \approx 0.7$. In contrast, when the response at Locality 2 is strong in Figure 5 (Bottom), there does not exist an adopted awareness constant value where a weak response at Locality 1 is better than a strong response at Locality 1 in terms of total outbreak size. Comparing Figures 5 (Top) and (Bottom),

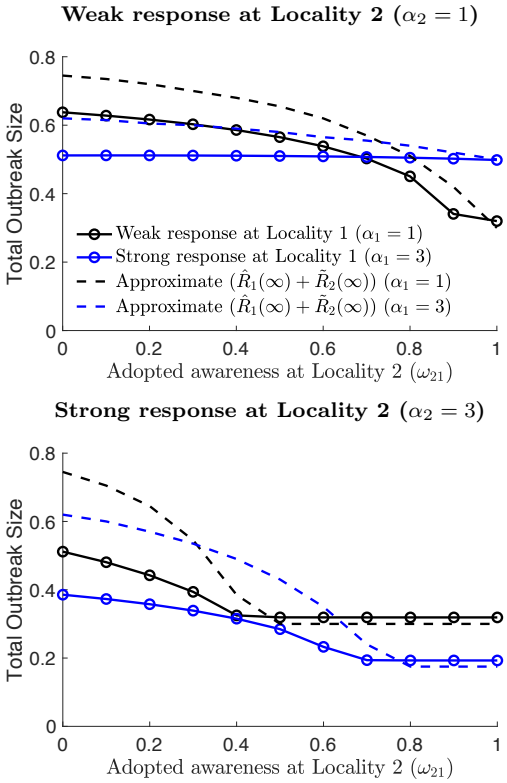

Figure 5: Total of outbreak sizes at localities 1 and 2 with respect to adopted awareness ω_{21}. (Top) Weak ($\alpha_2 = 1$) and (Bottom) strong ($\alpha_2 = 3$) responses at Locality 2. Mobility is set to $\lambda = 0.001\%$. Weak and strong response at Locality 1 correspond to ($\alpha_1 = 1$) and ($\alpha_1 = 3$), respectively. There exists a critical adopted awareness constant value in Top where the total outbreak size is lower in the scenario where both localities respond weakly compared to the scenario where Locality 1 has a strong response. The critical value for the adopted awareness constant value can be found by looking at the intersection of the solid black line with the solid blue line for the corresponding mobility value. When both localities respond strongly to the disease in Bottom figure, such a critical adopted awareness constant value does not exist.

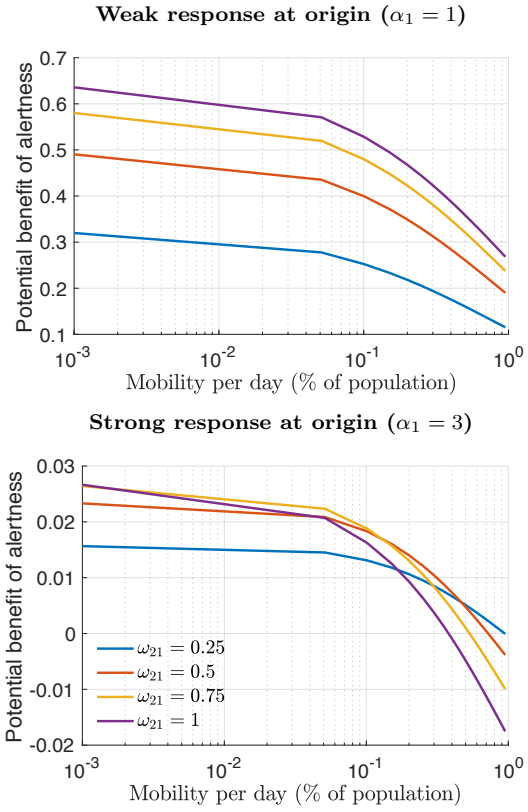

Figure 6: Benefit of adopted awareness with respect to mobility rates. (Top) Weak and (Bottom) strong responses at the origin. The strength of response at Locality 2 is weak $\alpha_2 = 1$. The benefit is measured as the reduction in final size with respect to the zero-adopted awareness constant scenario $\omega_{21} = 0$. Let $F_2(\omega_{21}, \lambda_{12})$ denote the final outbreak size at Locality 2 with respect to ω_{21} and λ_{12}. The benefit of alertness is defined as $F_2(0, \lambda_{12}) - F_2(\omega_{21}, \lambda_{12})$. Weak response at the origin, higher adopted awareness leads a smaller outbreak size at Locality 2 (Top). Given a strong response at the origin, higher adopted awareness can lead to higher outbreak sizes (Bottom). Strong response at the origin reduces the magnitude of the benefit of adopted awareness.

the total outbreak size is always lower in the Bottom, i.e., when the response at Locality 2 is strong. These observations indicate that we obtain the best outcome in terms of total outbreak size when both localities respond strongly, and Locality 2 has an adopted awareness constant value above the critical threshold ω_{21}^*.

In Figure 5, we also provide a theoretical approximation of the total outbreak size computed by adding the upper bound for the outbreak size in the origin ($\hat{R}_1(\infty)$) to the lower bound for the outbreak size at Locality 2 ($\tilde{R}_2(\infty)$). This total ($\hat{R}_1(\infty) + \tilde{R}_2(\infty)$) is neither an upper bound nor a lower bound. We see that the approximation error is mostly dominated by the error in the upper bound $\tilde{R}_2(\infty)$ for small values of the adopted awareness constant. The approximation is a lower bound of the total outbreak size for all adopted awareness values above the critical adopted awareness constant computed using (13)—see dashed lines in Figure 5(Bottom) lying below the corresponding solid lines.

3.5. Effects of mobility rates

Thus far, we have focused our analysis on the effects of adopted awareness given a slow mobility regime ($\lambda_{12} = 0.001\%$). As per the discussion in Section 3.1, the outbreak times between localities get closer as mobility increases. Given higher mobility rates, the cumulative number of cases at Locality 1 will be lower by the time disease begins to spread at Locality 2. Thus, we expect the benefit of adopted awareness at Locality 2 to be lower with increasing mobility.

In Figure 6, we analyze the effects of mobility rate on the outbreak size at Locality 2 in Figure 6. Specifically, we measure the benefit of adopted awareness (ω_{21}) by comparing the outbreak size at Locality 2 given a positive adopted awareness value $\omega_{21} > 0$ with the outbreak size when adopted awareness constant is zero, i.e., $\omega_{21} = 0$. Following the discussion above, given a positive adopted awareness constant value $\omega_{21} > 0$, the potential benefit of adopted awareness reduces as mobility increases. We see that the decrease in the benefit of preparedness is slow up until a mobility rate value. After a certain mobility value $\lambda_{12} \approx 0.05\%$, the decrease in the benefit of adopted awareness is sharper. Regardless, we observe that when the response at the origin is weak, it is better to have a higher level of adopted awareness—see Figure 6 (Top). The same cannot be said when the response at the origin is strong—see Figure 6 (Bottom). Indeed, lower adopted awareness values can yield smaller outbreak sizes at Locality 2 for high mobility. Moreover, we note that the benefit of alertness is weaker in magnitude, but more robust to increasing mobility rates, when the response at Locality 1 is stronger—compare y-axis values of Figure 6(Top) with (Bottom).

4. Conclusions

We developed a mathematical model to analyze the impact of social distancing efforts on disease

dynamics among interconnected populations. We assumed that social distancing efforts at a given location is a function of both disease prevalence within the population and outbreak dynamics at neighboring localities. Our analysis showed that it is beneficial to reduce travel between localities given the inability to detect asymptomatic infectious individuals (consistent with recent findings [1]). However, this benefit is contingent on how prepared neighboring localities are for the importation of cases. We used the term adopted awareness to determine the importance given to preparedness at neighboring localities. We assumed the preparedness at importing localities is an increasing function of the outbreak size at the origin. The increasing function assumption implied that neighboring localities increase their levels of preparedness as the severity of the disease at the origin increased. That is, as the severity of the outbreak at the origin increases, this triggers increased social distancing efforts at neighboring localities by local authorities making non-pharmaceutical interventions, e.g., declaring state of emergency, or issuing stay at home orders. We derived an upper bound on the outbreak size at importing localities as a function of the outbreak size at the origin and strength of response at the importing locality. Using this upper bound, we identified a critical threshold for adopted awareness weight that would eliminate the disease at importing localities.

It is not surprising that increased levels of preparedness reduces the outbreak size at localities neighboring the origin. However, the level of preparedness is dependent on the outbreak size at the origin. Thus, levels of preparedness increase at a locality when a neighboring locality has a larger outbreak size. Our results show that increased levels of preparedness at neighboring localities can yield lower total outbreak sizes even when the response at the origin is weak (Figure 5(Top)). The theoretical and numerical results mentioned above were under a low mobility regime in which there was a lead time for increased alertness levels at importing localities based on the outbreak size at the origin. We also find that adopted awareness is robust to variation in mobility, insofar as mobility remains relatively low (Figure 6 (Top)).

These findings imply that if there are multiple localities with outbreaks, the jurisdictions with less severe outbreaks should be looking at their worse-off neighbor rather than their best-off neighbor, and implementing social distancing measures accordingly. Given the continuing threat of COVID-19, the present study provides additional support for viewing pandemics in a connected, rather than isolated, context.

Appendix A. A lower bound on the outbreak size at the origin

We derive a close form solution for the outbreak size at the origin for the SEIR model in (1)-(4) when mobility is not included ($\lambda_{ij} = 0$). We modify the social distancing model at the origin (Locality 1) by

$$\hat{\beta}_1 = \beta \left(1 - E_1 + I_1 + R_1\right)^{\alpha_1} = S_1^{\alpha_1} \tag{A.1}$$

where we assumed $N_1 = 1$ to simplify notation. The social distancing model above assumes that individuals distance with respect to the cumulative number of cases including the exposed individuals which were not included in (5). We note that this assumption is for analysis purposes only and allows us to compute a lower bound on the outbreak size for the original model in (5).

We define the following quantity to be the weighted sum of exposed and infected individuals

$$Y(t) := E(t) + \frac{\mu}{\mu + \rho} I(t). \tag{A.2}$$

The force of infection is given by

$$\lambda(E_1, I_1) = \beta(E_1 + I_1). \tag{A.3}$$

Given the force of infection and the reproductive number (7) definitions, we can show that

$$\dot{Y} = \lambda(E_1, I_1)\left(S^{\alpha_1 + 1} - \frac{1}{\mathcal{R}_1}\right) \tag{A.4}$$

Then we have the constant of motion of the SEIR model ((1)-(4)) with the distancing model (A.1) as

$$Y(t) + S(t) + \frac{1}{\mathcal{R}_1}\frac{S(t)^{-\alpha_1}}{\alpha_1} = Y(0) + S(0) + \frac{S(0)^{-\alpha_1}}{\alpha_1} \tag{A.5}$$

for any t. In identifying the above constant of motion, we divide dY/dt by dS/dt in (1), simplify terms, and integrate the resultant relation from time 0 to t. These steps are similar to the steps used to establish speed-outbreak size relations for standard SEIR models without social distancing, e.g.,

see [18, 19]. Now letting $t \to \infty$ and using the fact that $S(0) = 1$, $Y(0) = 0$, $Y(\infty) = 0$, we obtain the speed of spread versus final size relation in (6) for $\alpha_1 > 0$.

The social distancing function in (A.1) includes exposed individuals. That is, we have $\tilde{\beta}_1(t) < \beta_1(t)$ for all t where $\beta_1(t)$ is as defined in (5). Thus the final size $R(\infty)$ in (8) is a lower bound on the outbreak size at the origin.

Appendix B. An upper bound for the outbreak size at the importing locality

Figures S1 and S2 show the lower bound on $S(\infty)$ obtained by solving (11). Top and bottom figures illustrate the change in the lower bound as a function of the strength of response at the origin. In accordance with the SEIR model (1)-(5), a strong response at the origin leads to a larger outbreak at Locality 2—compare diamond points in top and bottom in Figures S1 and S2. Similarly, the lower bound values $\tilde{S}_2(\infty)$ are lower in the bottom figures. Indeed, in both figures a weak response at the origin compounded by a strong response at Locality 2 guarantee that the outbreak does not happen in the Locality 2—see blue circles and diamonds in top figures.

The adopted awareness constant $(1 - \omega_{22})$ is smaller in Figure S1 than in Figure S2. We observe that the lower bound for $S(\infty)$ is tighter when ω_{22} is smaller. This is expected since as ω_{22} decreases the importance given to prevalence at Locality 2 $(I_2 + R_2)$ in (9). Thus the difference between the right hand sides of (9) and (10) decreases.

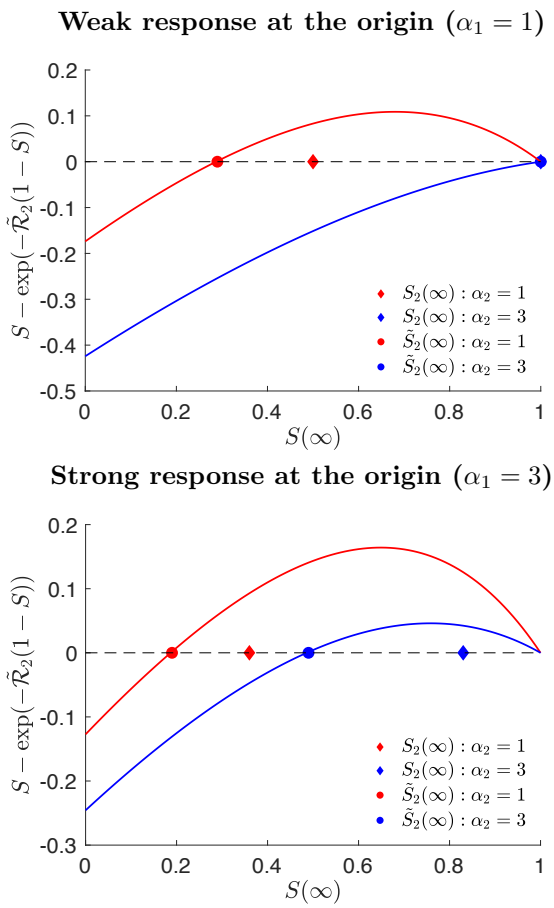

Figure S1: Lower bound values for $S(\infty)$. We assume low adopted awareness $\omega_{21} = 1/2$. We let $\mathcal{R}_1 = 2.5$ and $\lambda = 0.0001\%$. (Top) Weak and (Bottom) strong response at the origin. Lines correspond to the left hand side of (11). Circle dots show the solution to (11), i.e., intersection of lines with zero. Diamond dots are $S(\infty)$ values obtained by simulating the SEIR model in (1)-(4) with β_i in (5).

References

[1] R. Li, S. Pei, B. Chen, Y. Song, T. Zhang, W. Yang, J. Shaman, Substantial undocumented infection facilitates the rapid dissemination of novel coronavirus (sars-cov2), Science (2020).

[2] E. Javan, S. J. Fox, L. A. Meyers, Probability of current covid-19 outbreaks in all us counties, medRxiv (2020).

[3] M. Chinazzi, J. T. Davis, M. Ajelli, C. Gioannini, M. Litvinova, S. Merler, A. P. y Piontti, K. Mu, L. Rossi, K. Sun, et al., The effect of travel restrictions on the spread of the 2019 novel coronavirus (covid-19) outbreak, Science (2020).

[4] C. R. Wells, P. Sah, S. M. Moghadas, A. Pandey, A. Shoukat, Y. Wang, Z. Wang, L. A. Meyers, B. H. Singer, A. P. Galvani, Impact of international travel and border control measures on the global spread of the novel 2019 coronavirus outbreak, Proceedings of the National Academy of Sciences 117 (13) (2020) 7504–7509.

[5] Z. Du, L. Wang, S. Cauchemez, X. Xu, X. Wang, B. Cowling, L. Meyers, Risk for transportation of 2019 novel coronavirus disease from wuhan to other cities in china., Emerging infectious diseases 26 (5) (2020).

[6] M. U. Kraemer, C.-H. Yang, B. Gutierrez, C.-H. Wu, B. Klein, D. M. Pigott, L. du Plessis, N. R. Faria, R. Li, W. P. Hanage, et al., The effect of human mobility and control measures on the covid-19 epidemic in china, Science (2020).

[7] B. Klein, T. LaRocky, S. McCabey, L. Torresy, F. Privitera, B. Lake, M. U. Kraemer, J. S. Brownstein, D. Lazer, T. Eliassi-Rad, et al., Assessing changes in commuting and individual mobility in major metropolitan areas in the united states during the covid-19 outbreak (2020).

[8] D. J. Watts, R. Muhamad, D. C. Medina, P. S. Dodds, Multiscale, resurgent epidemics in a hierarchi-

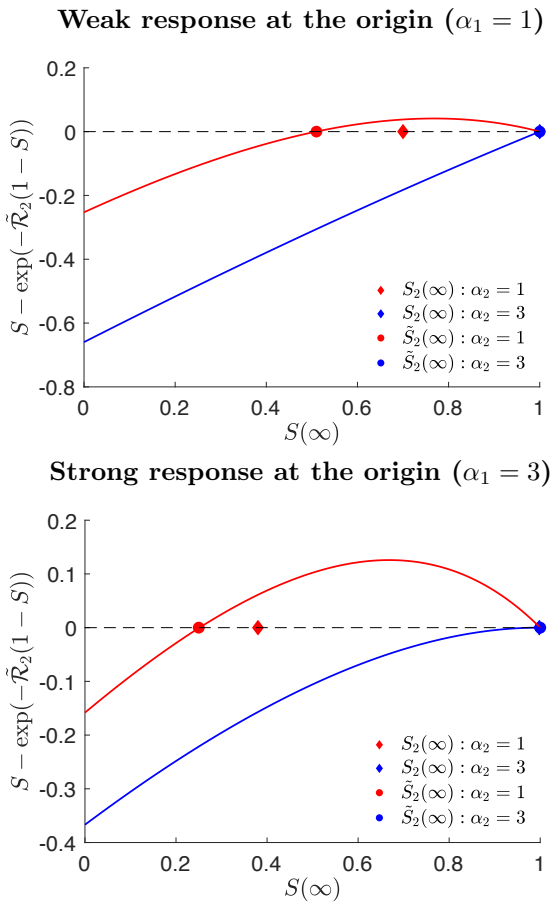

Figure S2: Lower bound values for $S(\infty)$. We assume high adopted awareness $\omega_{21} = 3/4$. We let $\mathcal{R}_1 = 2.5$ and $\lambda = 0.0001\%$. (Top) Weak and (Bottom) strong response at the origin. Lines correspond to the left hand side of (11). Circle dots show the solution to (11), i.e., intersection of lines with zero. Diamond dots are $S(\infty)$ values obtained by simulating the SEIR model in (1)-(4) with β_i in (5).

cal metapopulation model, Proceedings of the National Academy of Sciences 102 (32) (2005) 11157–11162.

[9] M. Salathé, J. H. Jones, Dynamics and control of diseases in networks with community structure, PLoS computational biology 6 (4) (2010).

[10] Z. Du, X. Wang, R. Pasco, M. Petty, S. J. Fox, L. A. Meyers, Covid-19 healthcare demand projections: 22 texas cities.

[11] V. Colizza, A. Vespignani, Invasion threshold in heterogeneous metapopulation networks, Physical review letters 99 (14) (2007) 148701.

[12] J. T. Wu, K. Leung, G. M. Leung, Nowcasting and forecasting the potential domestic and international spread of the 2019-ncov outbreak originating in wuhan, china: a modelling study, The Lancet 395 (10225) (2020) 689–697.

[13] X. He, E. H. Lau, P. Wu, X. Deng, J. Wang, X. Hao, Y. C. Lau, J. Y. Wong, Y. Guan, X. Tan, et al., Temporal dynamics in viral shedding and transmissibility of covid-19, medRxiv (2020).

[14] S. W. Park, D. M. Cornforth, J. Dushoff, J. S. Weitz, The time scale of asymptomatic transmission affects estimates of epidemic potential in the covid-19 outbreak, medRxiv (2020).

[15] K. Paarporn, C. Eksin, J. S. Weitz, J. S. Shamma, Networked SIS epidemics with awareness, IEEE Transactions on Computational Social Systems 4 (3) (2017) 93–103.

[16] C. Eksin, K. Paarporn, J. S. Weitz, Systematic biases in disease forecasting–the role of behavior change, Epidemics 27 (2019) 96–105.

[17] S. Funk, E. Gilad, C. Watkins, V. A. Jansen, The spread of awareness and its impact on epidemic outbreaks, Proceedings of the National Academy of Sciences 106 (16) (2009) 6872–6877.

[18] J. Ma, D. J. Earn, Generality of the final size formula for an epidemic of a newly invading infectious disease, Bulletin of mathematical biology 68 (3) (2006) 679–702.

[19] Z. Feng, Final and peak epidemic sizes for seir models with quarantine and isolation, Mathematical Biosciences & Engineering 4 (4) (2007) 675.

Acknowledgements

Joshua S. Weitz was supported, in part, by a grant from the Army Research Office (W911NF1910384). Martial-Ndeffo Mbah was, in part, supported by a grant from the National Science Foundation (BED 2028632)

Competing interests

Authors declare no competing interests.

Materials

The code is available at `https://github.com/ceyhuneksin/reacting_outbreaks_neighboring_localities`.